PHYSICAL REVIEW B **78**, 024506 (2008)

Quantum interference and weak localization effects in the interlayer magnetoresistance of layered metals

Malcolm P. Kennett[1] and Ross H. McKenzie[2]
[1]*Physics Department, Simon Fraser University, 8888 University Drive, Burnaby, British Columbia, V5A 1S6, Canada*
[2]*Physics Department, University of Queensland, Brisbane 4072, Australia*
(Received 8 April 2008; revised manuscript received 6 June 2008; published 3 July 2008)

Studies of angle-dependent magnetoresistance oscillations (AMRO) in the interlayer conductivity of layered metals have generally considered semiclassical electron transport. We consider a quantum correction to the semiclassical conductivity that arises from what can be described as an interlayer Cooperon. This correction depends on both the disorder potential within a layer and the correlations of the disorder potential between layers. We compare our results with existing experimental data on organic charge-transfer salts that are not explained within the standard semiclassical transport picture. In particular, our results may be applicable to effects that have been seen when the applied magnetic field is almost parallel to the conducting layers. We predict the presence of a peak in the resistivity as the field direction approaches the plane of the layers. The peak can occur even when there is weakly incoherent transport between layers.

DOI: 10.1103/PhysRevB.78.024506 PACS number(s): 74.72.−h, 71.18.+y, 72.10.−d, 74.70.Kn

I. INTRODUCTION

Angle dependent magnetoresistance oscillations (AMRO) are valuable tools for the investigation of properties of layered metals such as organic and cuprate superconductors. The dependence of the interlayer magnetoresistance on the direction of the magnetic field has been used to map out three-dimensional Fermi surfaces, sometimes in exquisite detail in a diverse range of layered metals. These include organic charge-transfer salts,[1] strontium ruthenates,[2,3] semiconductor superlattices,[4] monophosphate tungsten bronze,[5] and an overdoped cuprate.[6–8] More recent developments have extended this to allow one to not only determine the anisotropies in the Fermi surface, but also the anisotropy of scattering on the Fermi surface.[7–13]

In addition to the shape of the Fermi surface, the coherence of interlayer transport in layered metals has been a complicated and controversial issue.[14] In order for AMRO to be observable, only coherence between neighboring layers is required, i.e., weakly incoherent transport, and for almost all angles, this leads to AMRO that is equivalent to fully coherent transport (i.e., there is a three-dimensional Fermi surface) perpendicular to the planes.[11,15] In general, the two situations can be distinguished in transport measurements only if there is a coherence peak in the resistivity for fields close to parallel to the layers. In this work, we show that quantum interference effects can also lead to a peak in the resistivity at fields close to parallel to the layers, for weakly incoherent transport. However, this peak can be distinguished from the coherence peak by its magnetic-field and temperature dependence, which is determined by the length scales and time scales over which quantum coherence is destroyed.

The peak in the resistivity that we find for parallel fields arises from a contribution to interlayer conductivity in a magnetic field $\mathbf{B}=B(\sin\theta\cos\phi,\sin\theta\sin\phi,\cos\theta)$ in layered metals which is a quantum correction to existing semiclassical transport formulae.[11,15] There has been previous work in this direction,[16–22] but this either focused on weak localization in anisotropic metals, or did not consider the magnetic-field configurations relevant for AMRO. Our work is motivated by experiments in which deviations from conventional AMRO are seen.[13,23,24] The particular deviations of interest are weak localization-like peaks at angles near $\theta=90°$.[23] We calculate the quantum contribution to the interlayer resistivity and show that it behaves in a similar way in a perpendicular magnetic field to the Cooperon in a two-dimensional electron system. We also show that a peak for parallel magnetic fields emerges naturally for reasonable choices of relevant materials properties, leading us to suggest that this physics is relevant for a number of recent experiments.

Our main results are an expression for the interlayer Cooperon correction to interlayer conductivity and asymptotic expressions for magnetic fields that are close to parallel to the conducting layers. We demonstrate the presence of a small peak in the resistivity for such fields and discuss the characteristic behavior with temperature and perpendicular magnetic field that allow this feature to be distinguished from coherence peaks at similar field orientations.

We note that the calculations we consider here may also be of interest to those considering weak localization effects in bilayer or multilayer graphene,[27,28] semiconductor double quantum wells,[22] semiconductor quantum wells with intersubband scattering[29] and superlattices.[21]

The paper is structured as follows: in Sec. II we briefly review the physics associated with magnetoresistance due to weak localization and discuss the experiments that motivate our calculations. In Sec. III we give details of our calculations and results, and in Sec. IV we discuss the consequences of our results for the interpretation of AMRO experiments, particularly on the issue of coherent versus incoherent interlayer transport.

II. MAGNETORESISTANCE DUE TO WEAK LOCALIZATION

The theory of weak localization in two-dimensional electron systems (2DES) is well established. Nevertheless, to

connect our calculations to experimental data showing unusual peaks in AMRO, we briefly discuss the key physical quantities that determine the magnitude of weak localization effects in 2DES.[30,31] We then summarize our main results and review relevant experimental data. The conductivity of a 2DES in a perpendicular magnetic field $B_\perp$ at temperature T can be written as

$$\sigma(B_\perp,T) = \sigma_{cl}(B_\perp,T) + \delta\sigma(B_\perp,T), \tag{1}$$

where σ_{cl} is the semiclassical conductivity and $\delta\sigma$ is associated with quantum interference effects and weak localization. The relative magnitude of the two terms is of order $\delta\sigma/\sigma_{cl} \sim 1/k_F\ell$, where k_F is the Fermi wave vector and $\ell = v_F\tau$ is the elastic mean-free path, with v_F the Fermi velocity and τ the elastic-scattering time. Quantum effects are enhanced by increased disorder, which reduces $k_F\ell$. At low temperatures in zero magnetic field

$$\delta\sigma(T) \simeq -\frac{e^2}{2\pi^2\hbar}\ln\left(\frac{\tau_\phi(T)}{\tau}\right), \tag{2}$$

where τ_ϕ is the inelastic-scattering time, which includes all inelastic processes, e.g., electron-electron and electron-phonon scattering. Generally, $1/\tau_\phi \sim T^p$, with $p>0$, so the resistivity diverges logarithmically with decreasing T.

The temperature dependent magnetic-field scale (the phase breaking field) where quantum interference effects are destroyed is ($D=\frac{1}{2}v_F^2\tau$ is the diffusion constant)

$$B_\phi(T) = \frac{\hbar}{4eD\tau_\phi(T)} = \frac{\hbar}{2e\ell^2}\frac{\tau}{\tau_\phi(T)}. \tag{3}$$

Suppression of quantum interference leads to negative magnetoresistance which is quadratic in $B_\perp$ for $B_\perp \ll B_\phi(T)$.[30–33] When $B_0=\frac{\hbar}{4eD\tau} \gg B_\perp$ and $\tau_\phi \gg \tau$ [i.e., $B_0 \gg B_\phi(T)$], the change in the quantum contribution to the conductivity due to the magnetic field can be written in terms of $\psi(z)$, the digamma function,

$$\begin{aligned}\Delta\sigma &\equiv \sigma(B_\perp) - \sigma(B_\perp = 0)\\ &= \frac{e^2}{2\pi^2\hbar}\left\{\ln\left[\frac{B_\perp}{B_\phi(T)}\right] + \psi\left[\frac{1}{2}+\frac{B_\phi(T)}{B_\perp}\right]\right\},\\ &\simeq \frac{e^2}{48\pi^2\hbar}\left[\frac{B_\perp}{B_\phi(T)}\right]^2.\end{aligned} \tag{4}$$

Equation (4) can be used to fit experimental data for the magnetoconductivity with one free parameter, $\tau_\phi(T)$. For thin metallic films and semiconductor heterostructures, this has proven to be a powerful method for determining the absolute value and temperature dependence of the inelastic-scattering rate.[31,34]

A. Summary of results

In this paper, we calculate the analog of weak localization corrections to in-plane conductivity in the interlayer resistance of layered metals. Our calculations establish the following:

(1) When the temperature is low enough that $\tau_\phi \gg \tau$, and $B_\perp = 0$, there will be a small increase in the interlayer resistivity which is approximately logarithmic in temperature.

(2) At low temperatures, there will be a small negative magnetoresistance on the scale of $B_\perp \sim B_0$.

(3) Even when the field parallel to the layers $B_\parallel$ is large, there will still be a contribution to the resistance due to weak localization similar to that which occurs in zero field. As the field is tilted at an angle $\delta\theta$, slightly away from the layers, there is a small perpendicular field, $B_\perp \simeq B\delta\theta$. Consequently, a graph of the interlayer resistance versus θ will have a narrow peak at $\theta=\pi/2$, with a width which is an inverse power of B when $\tau_\phi > \tau$. The field B_a [defined in Eq. (30)] sets the field scale that cuts off the logarithmic divergence; the temperature dependence of B_a implies that the height and width of the peak are also temperature dependent. The height of the peak relative to the background magnetoresistance will only depend weakly on the strength of the field parallel to the layers when $B_\parallel > B_p$ [defined in Eq. (5)].

(4) The resistance peak is quite distinct from the "coherence" peak which can occur at $\theta=\frac{\pi}{2}$ if there is coherent interlayer transport (i.e., a three-dimensional Fermi surface).[1,15] The coherence peak only exists at very high fields $[B_\parallel \gg m^* k_F c\sqrt{\epsilon_F/t_\perp}/e\tau(T)]$, has a width $\delta\theta = 2k_F c(t_\perp/\epsilon_F)$ which is independent of temperature and field, and its height relative to the background scales with B and τ.[1,35]

(5) There are two regimes of parallel field, separated by an intermediate field scale,

$$B_p \equiv \frac{\hbar}{ec\ell}. \tag{5}$$

For $B_\parallel \ll B_p$, the corrections to the conductivity are essentially independent of $B_\parallel$, whereas the semiclassical background does depend on $B_\parallel$. For $B_\parallel \gtrsim B_p$, the correction to the conductivity has the same $B_\parallel$ dependence as the semiclassical contribution, so that the relative resistivity correction (i.e., the shape of the peak) becomes a function of $B_\perp$ only near $\theta=\frac{\pi}{2}$.

B. Brief review of experimental results

There are several layered metallic systems for which peaks in the interlayer resistance have been observed for magnetic fields that are close to parallel to the conducting layers. We review whether such peaks are likely to be weak localization or coherence peaks.

1. β''-(BEDT-TTF)$_4$AM(C$_2$O$_4$)$_3$Y

A class of layered metals where weak localizationlike peaks have been observed[26] is the family of organic charge-transfer salts β''-(BEDT-TTF)$_4$AM(C$_2$O$_4$)$_3$Y, where Y is a solvent molecule, M=Ga, Cr, Fe, and $A=H_3O^+$. These materials have several features unlike other organic charge-transfer salts that make them more likely to exhibit weak localization effects: (a) smaller Fermi wave vector, (b) stronger disorder, [both (a) and (b) reduce $k_F\ell$], and (c) almost 3/4 filling, which enhances the strong electronic correlations which narrow the electronic bands, reducing the Fermi energy ϵ_F.[36]

The small Fermi surface has been established from Shubnikov–de Haas (SdH) oscillations with period 330 T, corresponding to a circular Fermi surface with $k_F=1$ nm^{-1}. The corresponding Fermi-surface area is an order of magnitude smaller than in many ET materials. This arises because the β'' crystal structure leads to four bands, three of which are almost completely filled,[38] so the Fermi energy is near the band edge. The effective mass associated with these SdH oscillations is close to one free-electron mass and $\epsilon_F \sim 35$ meV.

Evidence for strong disorder is seen in the Dingle temperatures of 1–4 K estimated from SdH oscillations, which are up to an order of magnitude larger than the cleanest organic charge-transfer salts.[1] There is significant structural disorder, especially in the anion layers.[25] This has the consequence that the ratio of the resistivity at room temperature to that at low temperatures is of order one. In contrast, in many metallic organic charge-transfer salts, this ratio is as large as one thousand.[39]

In both the $M=$Ga and Cr ($Y=C_2H_2Cl_2$) materials in zero field, the interlayer resistivity increases approximately logarithmically with temperature below about 20 K with a total change of about 1% between 1 and 20 K.[26] At a temperature of 1.5 K, perpendicular fields of about 0.2 and 2 T destroy this feature in the $M=$Ga and $M=$Cr materials, respectively. Furthermore, as the field is tilted toward the plane of the layers, there is a small peak in the interlayer resistance versus angle for both the $M=$Cr and $M=$Ga material at $\theta=\pi/2$. The width of this peak, $\delta\theta$ (in radians), has a field dependence $B_x/B_\perp$, with $B_x \sim 0.25$ T between about 3 and 14 T for the $M=$Cr material.[26] The weak localization peak at $\theta=0$ also occurs on the scale of B_x. The magnitude of the peak is about 0.3% of the background magnetoresistance and depends weakly on the parallel field. As the temperature increases from 0.7 to 3 K, the peak becomes broader and smaller, and is not visible at 6 K, whereas the background magnetoresistance changes little in the same temperature range.

2. α-[(ET)$_{1-x}$(BETS)$_x$]$_2$KHg(SCN)$_4$

In α-[(ET)$_{1-x}$(BETS)$_x$]$_2$KHg(SCN)$_4$ with $x \simeq 0.03$, the resistance versus temperature curve shows an upturn below about 5 K.[40] About 10% of this growth can be suppressed with a magnetic field. The peak in the resistance that occurs at $\theta=\pi/2$ is about 50 times broader than the coherence peak that occurs in clean α-(ET)$_2$KHg(SCN)$_4$ samples at fields of order a few tesla.[24] For low fields, up to 1.5 T, the shape of the peak depends only on $B_\perp$, as would be expected for weak localization, and at higher fields, the peak becomes broader. The high-field behavior is not captured in our theory which may be related to approximations we use that should break down at very large fields (e.g., 15 T in this case).

3. κ-(BEDT-TTF)$_2$Cu(NCS)$_2$

The magnitude and temperature dependence of the inelastic-scattering rate in κ-(BEDT-TTF)$_2$Cu(NCS)$_2$ was recently determined using AMRO.[13] The data was fit to

$$\frac{1}{\tau(T)} = \frac{1}{\tau_{11}} + AT^2, \tag{6}$$

with $\tau_{11} \simeq 3$ ps and $A \simeq 0.006$ ps^{-1} K^{-2}. This temperature dependence is consistent with that of the dc resistivity in many organic charge-transfer salts.[41] The first term is associated with elastic scattering due to disorder and the quadratic temperature dependence can be associated with inelastic scattering due to electron-electron interactions. The ratio of the inelastic-scattering time $\tau_\phi(T)$ to the intralayer elastic-scattering time is $\tau_\phi/\tau_{11}=50(\mathrm{K}/T)^2$. Thus, as the temperature increases from 1 to 20 K, the ratio decreases from 50 to 0.1.

We suggest that weak localization may be the origin of the feature near $\theta=\frac{\pi}{2}$ that Singleton *et al.*[13] assigned to the coherence peak. The peak width appears to broaden with increasing temperature [as would be expected for decreasing τ_ϕ, and hence increasing $B_\phi(T)$]. In earlier data on the same material,[23] the peak height drops with increasing temperature and the peak width increases with increasing temperature. For an inelastic-scattering rate that increases with temperature, this as would be expected for weak localization, since $B_\phi(T)$ increases with increasing temperature and the width of the peak goes as B_ϕ, while its height should increase logarithmically with temperature.

4. Intercalated graphite

A peak near parallel field has also been seen in intercalated graphite materials which display unusual inverted AMRO.[42] However, the width of the peak appears to be independent of magnetic field which would tend to argue against weak localization effects.

III. MODEL AND CALCULATIONS

A. Interlayer charge transport

In previous work,[11] we considered the AMRO that arises when there is an anisotropic Fermi surface and anisotropic scattering in two different limits. These two limits were the limit of coherent interlayer transport and the limit of weakly incoherent interlayer transport in which there is hopping between adjacent layers. We shall not consider anisotropy in the Fermi surface, scattering, or the interlayer hopping here, as these are additional complications beyond the physics that is our main interest. For isotropic weakly incoherent interlayer transport the Hamiltonian describing interlayer charge transport is

$$\mathcal{H} = t_\perp \sum_{i,j=1,2} [c_i^\dagger c_j + \mathrm{H.c.}], \tag{7}$$

where $t_\perp$ is the interlayer hopping integral. We assume that we are in weakly incoherent regime such that

$$t_\perp \ll \frac{1}{\tau}. \tag{8}$$

There is no observable difference in the AMRO between the coherent and weakly incoherent models of interlayer transport except for polar angles of the magnetic field very close

to 90°, corresponding to a magnetic field parallel to the planes.[11,15] The interlayer conductivity that is deduced from such a hopping Hamiltonian is:[15]

$$\sigma_\perp = \frac{e^2 c t_\perp^2}{\hbar \pi L^2} \int d^2\mathbf{r}_1 \int d^2\mathbf{r}_2 \langle G_1^R(\mathbf{r}_1,\mathbf{r}_2) G_2^A(\mathbf{r}_2,\mathbf{r}_1) + G_1^A(\mathbf{r}_1,\mathbf{r}_2) G_2^R(\mathbf{r}_2,\mathbf{r}_1)\rangle, \quad (9)$$

where c is the interlayer spacing, L is the sample size, and $G_i^{R(A)}$ is the retarded (advanced) Green's function in layer i. The angle brackets $\langle \ldots \rangle$ indicate an average over disorder. Generically, in calculating the disorder-averaged conductivity, there are two classes of diagrams to consider, the ladder diagrams that lead to the "Diffuson," and the maximally crossed diagrams that lead to the "Cooperon."[30,31] In our previous work, we found that the AMRO from weakly incoherent interlayer transport could be derived using a "Diffuson-like" equation.[11] We expect that there should also be a contribution to the interlayer conductivity from a "Cooperon-like" process, that will have a different magnetic-field dependence to the Diffuson term due to their differing time-reversal properties. It is this question that we address in this paper, and we find that indeed, an extra quantum correction to the interlayer conductivity is generated. Moreover, it has distinct experimental signatures.

B. Impurity correlations in a layered metal

We now discuss the properties of the probability distribution for impurities in a layered metal, and their consequences for impurity correlations. We assume that the probability distribution $p(\mathbf{r})$ for the locations of impurities can be factorized into separate distributions describing the distributions parallel $[p_\parallel(x,y)]$ and perpendicular $[p_z(z)]$ to the layers[21]

$$p(\mathbf{r}) = p_\parallel(x,y) p_z(z).$$

We assume that an individual impurity (or lattice defect) located at $\mathbf{R}$ has a potential $V_{\mathrm{imp}}(\mathbf{r}-\mathbf{R})$ associated with it, and that

$$\langle V(\mathbf{r})\rangle = n_i \int d^3\mathbf{r}' p(\mathbf{r}') V_{\mathrm{imp}}(\mathbf{r}-\mathbf{r}') = 0.$$

Correlations in the random potential take the form

$$\langle V(\mathbf{r}) V(\mathbf{r}')\rangle = n_i \int d^3\mathbf{r}'' p(\mathbf{r}'') V_{\mathrm{imp}}(\mathbf{r}-\mathbf{r}'') V_{\mathrm{imp}}(\mathbf{r}'-\mathbf{r}'') = n_i \int d^2\mathbf{r}'' p_\parallel(x'',y'') \int dz'' p_z(z'') \times V_{\mathrm{imp}}(\mathbf{r}-\mathbf{r}'') V_{\mathrm{imp}}(\mathbf{r}'-\mathbf{r}''). \quad (10)$$

We shall assume that there is a uniform distribution of impurities in the planes parallel to the conducting layers, i.e., $p_\parallel(x,y)=\frac{1}{L^2}$, where L is the sample size. All structure in the impurity distribution is thus in p_z which will tend to be peaked in the regions in between conducting layers. We note that periodicity and inversion symmetry imply that $p(z) = p(-z) = p(z+c)$.

We give a layer index to the random potential V_j depending on whether the electron z coordinate lies in layer 1 or layer 2. There will then be two important types of disorder correlations, $\langle V_i(\mathbf{r}') V_j(\mathbf{r})\rangle$, where i and j are layer indices. First, correlations within a single layer, $\langle V_1(\mathbf{r}') V_1(\mathbf{r})\rangle$, contribute to the in-plane elastic-scattering rate and appear in the disorder-averaged single layer Green's functions. Second, correlations between layers, $\langle V_1(\mathbf{r}') V_2(\mathbf{r})\rangle$, are relevant for interlayer conductivity. The corresponding expressions are (using the symmetry properties of p_z):

$$\langle V_1(\mathbf{r}') V_1(\mathbf{r})\rangle = \frac{n_i}{L^2} \int d^2\mathbf{r}'' \int_{-c/2}^{c/2} dz p_z(z) \times V_{\mathrm{imp}}(\mathbf{r}'-\mathbf{r}'',z) V_{\mathrm{imp}}(\mathbf{r}-\mathbf{r}'',z), \quad (11)$$

$$\langle V_1(\mathbf{r}') V_2(\mathbf{r})\rangle = \frac{n_i}{L^2} \int d^2\mathbf{r}'' \int_0^c dz p_z(z) \times V_{\mathrm{imp}}(\mathbf{r}'-\mathbf{r}'',c-z) V_{\mathrm{imp}}(\mathbf{r}-\mathbf{r}'',-z), \quad (12)$$

C. Elastic scattering times in a layered metal

In order to be clearer as to what we mean by an interlayer Cooperon, we now discuss the nature of the disorder potential and the associated elastic-scattering times. We shall assume that disorder correlations can be represented as delta correlated, i.e.,

$$\langle V_i(\mathbf{r}') V_j(\mathbf{r})\rangle = \bar{U}_{ij}^2 \delta(\mathbf{r}-\mathbf{r}'), \quad (13)$$

where $i,j=1,2$. It is useful to rewrite

$$\bar{U}_{ij}^2 = \frac{\hbar^3}{m^* \tau_{ij}} = \frac{\hbar}{2\tau_{ij}} \frac{1}{\pi N_s}, \quad (14)$$

where $N_s = \frac{m^*}{2\pi\hbar^2}$ is the two-dimensional density of states, not including spin degeneracy, and m^* is the effective mass. Thus, there are two distinct elastic-scattering times associated with the disorder. $\tau_{11}=\tau_{22}$ is the scattering time for in-plane elastic scattering, while $\tau_{12}=\tau_{21}$ is the scattering time corresponding to scattering correlations between adjacent layers. If the impurities are all equidistant between the layers, i.e., $p(z)$ has a maximum at $z=\pm c/2$, then we will have $\tau_{11} \simeq \tau_{12}$, whereas if the impurities are located in the conducting layers, we expect $\tau_{11} < \tau_{12}$.

We note that previous theoretical treatments of AMRO have not considered the possible role of disorder correlations between neighboring layers which could also modify the semiclassical interlayer conductivity.[43]

D. Interlayer Cooperon in the absence of magnetic field

The conductivity diagrams corresponding to the situation we consider are as shown in Fig. 1. Following the treatment of the two-dimensional problem by Rammer[30] or Datta,[31] we can write the correction to the interlayer conductivity from the Cooperon (in zero magnetic field) as

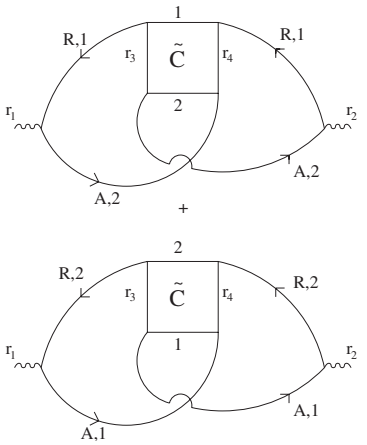

FIG. 1. Diagrams for the quantum correction to the interlayer conductivity. Note that $\tilde{C}=\bar{U}_{12}^2 C$ is related to the interlayer Cooperon. This is a diagrammatic representation of Eq. (15).

$$\delta\sigma_{\perp}^{C}=\frac{e^2ct_{\perp}^2}{\pi\hbar L^2}\int d\epsilon\left(-\frac{\partial f}{\partial\epsilon}\right)\int d^2\mathbf{r}_1\int d^2\mathbf{r}_2\int d^2\mathbf{r}_3\int d^2\mathbf{r}_4$$
$$\times\{G_1^R(\mathbf{r}_1,\mathbf{r}_3)G_1^R(\mathbf{r}_4,\mathbf{r}_2)\bar{U}_{12}^2C_{12}(\mathbf{r}_3,\mathbf{r}_4)$$
$$\times G_2^A(\mathbf{r}_2,\mathbf{r}_3)G_2^A(\mathbf{r}_4,\mathbf{r}_1)+G_1^A(\mathbf{r}_4,\mathbf{r}_1)G_1^A(\mathbf{r}_2,\mathbf{r}_3)$$
$$\times\bar{U}_{12}^2C_{21}(\mathbf{r}_3,\mathbf{r}_4)G_2^R(\mathbf{r}_1,\mathbf{r}_3)G_2^R(\mathbf{r}_4,\mathbf{r}_2)\},\tag{15}$$

where $\tilde{C}=\bar{U}_{12}^2C$ is the Cooperon (Fig. 2). The diagrammatic expansion of the Cooperon in Fig. 2 implies the following equation for the interlayer Cooperon:

$$C_{12}(\mathbf{r},\mathbf{r}')=\delta(\mathbf{r}-\mathbf{r}')+\int d^2\mathbf{r}''\tilde{J}_{12}^{C}(\mathbf{r},\mathbf{r}'')C_{12}(\mathbf{r}'',\mathbf{r}'),\tag{16}$$

where

$$\tilde{J}_{12}^{C}(\mathbf{r},\mathbf{r}')=\bar{U}_{12}^2G_1^R(\mathbf{r},\mathbf{r}')G_2^A(\mathbf{r},\mathbf{r}'),\tag{17}$$

is the Cooperon insertion. We can Taylor expand $C_{12}(\mathbf{r}'',\mathbf{r})$ and obtain[30] the following generalization of the standard equation for the Cooperon in the experimentally relevant limit that the in-plane elastic-scattering time, τ_{11}, is much less than the inelastic-scattering time, $\tau_{11}\ll\tau_{\phi}$:

$$\left\{\frac{1}{\tau_a}-D_a\nabla_r^2\right\}C_{12}(\mathbf{r},\mathbf{r}')=\frac{1}{\tau_{11}}\delta(\mathbf{r}-\mathbf{r}'),\tag{18}$$

which has the same form as the equation for the intralayer Cooperon, except that the diffusion constant is

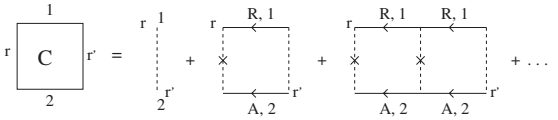

FIG. 2. Diagrams that give rise to the "interlayer Cooperon," described by Eq. (16). Neighboring layers are indicated as 1 and 2. A and R denote advanced and retarded Greens functions, respectively.

$$D_a=\frac{\tau_{11}}{\tau_{12}}D_0=\frac{v_F^2\tau_{11}^2}{2\tau_{12}},\tag{19}$$

and the scattering rate which destroys the interlayer Cooperon is

$$\frac{1}{\tau_a(T)}=\frac{1}{\tau_{11}}-\frac{1}{\tau_{12}}+\frac{1}{\tau_{\phi}(T)}.\tag{20}$$

In contrast, the first two terms do not appear for the intralayer Cooperon. For a general impurity potential, $\tau_{11}<\tau_{12}$ and so the effective dephasing rate will have a nonzero value at zero temperature. The structure of this expression has some similarities to what occurs with spin-orbit scattering[32] or intervalley scattering.[27]

E. Interlayer Cooperon in the presence of a magnetic field

In the presence of a magnetic field parallel to the layers, we note that Green's functions in layers 1 and 2 are related by a gauge factor[15]

$$G_1(\mathbf{r},\mathbf{r}')=\exp\left[\frac{iec}{2\hbar}\mathbf{B}_{\parallel}\cdot(\mathbf{r}-\mathbf{r}')\right]G_2(\mathbf{r},\mathbf{r}'),$$

and that Green's functions can be written as a gauge dependent phase multiplying a gauge-invariant piece:

$$G(\mathbf{r},\mathbf{r}')=\exp\left(\frac{ie}{\hbar}\int_{\mathbf{r}'}^{\mathbf{r}}\mathbf{A}_{\perp}\cdot d\mathbf{l}\right)G_0(\mathbf{r},\mathbf{r}'),$$

where $\mathbf{A}_{\perp}$ is the vector potential associated with the perpendicular magnetic field $\mathbf{B}_{\perp}$ and then

$$\tilde{J}_{12}^{C}(\mathbf{r},\mathbf{r}')\to\tilde{J}_{12}^{C,0}(\mathbf{r},\mathbf{r}')\exp\left[\frac{iec}{2\hbar}\mathbf{B}_{\parallel}\cdot(\mathbf{r}-\mathbf{r}')\right]$$
$$\times\exp\left[\frac{2ie}{\hbar}(\mathbf{r}-\mathbf{r}')\cdot\mathbf{A}_{\perp}(\mathbf{r})\right].\tag{21}$$

This allows us to generalize Eq. (18), as follows. We choose the Landau gauge to determine the perpendicular field, make a gauge transformation to eliminate the $\mathbf{B}_{\parallel}$ dependent term, and end up with an equation for $C'_{12}(\mathbf{r},\mathbf{r}')=\exp[\frac{iec}{2\hbar}\mathbf{B}_{\parallel}\cdot(\mathbf{r}-\mathbf{r}')]C_{12}(\mathbf{r},\mathbf{r}')$ which is (when we approximate $\tilde{J}_{12}^{C,0}$ by its zero-field value)

$$\left\{\frac{1}{\tau_a}-D_a\left(\nabla_r-\frac{2ie}{\hbar}\mathbf{A}_{\perp}\right)^2\right\}C'_{12}(\mathbf{r}',\mathbf{r})=\frac{1}{\tau_{11}}\delta(\mathbf{r}-\mathbf{r}').\tag{22}$$

Note that the approximation of $\tilde{J}_{12}^{C,0}$ by its zero-field value implies that for high enough fields, our expressions will not be applicable. Now, $C_{12}(\mathbf{r}_3,\mathbf{r}_4)\simeq C_{12}(\mathbf{r}_3,\mathbf{r}_3)$, since the Cooperon is dominated by loops of time-reversed paths, and in a perpendicular magnetic field $B_{\perp}$, the solution of equations of the form of Eq. (22) is well known.[30,33] For our parameters this is

$$C'_{12}(\mathbf{r}_3,\mathbf{r}_3) = \frac{2eB_\perp}{2\pi\hbar}\sum_{n=0}^{n_{\max}} \frac{1}{4D_a|e|B_\perp \frac{\tau_{11}}{\hbar}\left(n+\frac{1}{2}\right)+\frac{\tau_{11}}{\tau_a}}, \tag{23}$$

with $n_{\max} \simeq l_B^2/\ell^2$,[30] where $\ell = v_F\tau_{11}$ is the in-plane mean-free path.

To calculate the conductivity, we need to take into account the phase acquired by the propagators due to the vector potential differing in each layer. Thus, considering the first term in the conductivity (since the second term is its complex conjugate) and switching to momentum space propagators the expression simplifies to:

$$\delta\sigma_\perp^C = 2\,\mathrm{Re}\left[\frac{e^2ct_\perp^2\bar{U}_{12}^2}{\pi\hbar L^2}\int\frac{d^2\mathbf{k}_1}{(2\pi)^2}\frac{d^2\mathbf{k}_2}{(2\pi)^2}G^R(\mathbf{k}_1)G^R(\mathbf{k}_2) \times G^A\left(\mathbf{k}_1+\frac{ec}{2\hbar}\mathbf{B}_\parallel\right)G^A\left(\mathbf{k}_2+\frac{ec}{2\hbar}\mathbf{B}_\parallel\right) \times \int d\mathbf{r}_3\int d\mathbf{r}_4 C_{12}(\mathbf{r}_3,\mathbf{r}_4)e^{i(\mathbf{k}_1+\mathbf{k}_2)\cdot(\mathbf{r}_3-\mathbf{r}_4)}\right]. \tag{24}$$

Making use of Eq. (23) we obtain the expression

$$\delta\sigma_\perp^C = \frac{2ce^2t_\perp^2\bar{U}_{12}^2}{\pi\hbar}\left(\frac{eB_\perp}{\pi\hbar}\right)\sum_{n=0}^{n_{\max}}\frac{\mathrm{Re}[F(\mathbf{B}_\parallel)]}{4D_a|e|B_\perp\frac{\tau_{11}}{\hbar}\left(n+\frac{1}{2}\right)+\frac{\tau_{11}}{\tau_a}}. \tag{25}$$

In the Appendix we show that for $ecB_\parallel \ll \hbar k_F$ (the experimentally relevant limit)

$$\mathrm{Re}[F(\mathbf{B}_\parallel)] \simeq -\frac{2m^*\tau_{11}^3}{\hbar^5}f\left(\frac{e}{\hbar}B_\parallel c\ell\right), \tag{26}$$

where

$$f(x) \equiv \frac{1+\frac{x^2}{8}}{\left(1+\frac{x^2}{4}\right)^{3/2}}. \tag{27}$$

Note that $f(x) \simeq 1-\frac{x^2}{4}$ for $x \ll 1$ and $f(x) \simeq \frac{1}{x}$ for $x \gg 1$.

We can rewrite Eq. (25) in a similar form to the magnetoresistance in a thin film[33] using the properties of the digamma function $\psi(x)$,[44] which is related to the sum we have obtained via

$$\psi(x+n+1)-\psi(x) = \sum_{m=0}^{n}\frac{1}{x+m}.$$

Hence, we obtain

$$\delta\sigma_\perp^C(B_\perp) = -\sigma_1\left[\psi\left(\frac{B_a}{B_\perp}+n_{\max}+\frac{3}{2}\right)-\psi\left(\frac{B_a}{B_\perp}+\frac{1}{2}\right)\right],$$

$$\simeq \sigma_1\left[\ln\left(\frac{B_\perp}{B_0}\right)+\psi\left(\frac{1}{2}+\frac{B_a}{B_\perp}\right)\right], \tag{28}$$

with $B_0 = \frac{\hbar}{e\ell^2}$, and

$$\sigma_1(B_\parallel) = \frac{2ce^2t_\perp^2}{\pi^2\hbar^3v_F^2}f\left(\frac{B_\parallel}{B_p}\right), \tag{29}$$

where B_p is the field scale defined in Eq. (5).

The magnetic-field dependence is of the same form as that for the weak localization correction to the intralayer conductivity, Eq. (4), with $B_\phi(T)$ replaced by the magnetic-field scale

$$B_a(T) \equiv \frac{\hbar}{4eD_a\tau_a(T)}, \tag{30}$$

where τ_a is given by Eq. (20). Consequently, we note that unlike the phase breaking field associated with the intralayer conductivity that in general this quantity will be nonzero even at zero temperature. In the absence of a perpendicular magnetic field, the interlayer Cooperon correction to conductivity reduces to

$$\delta\sigma_\perp^C(B_\perp=0,T) = \sigma_1\ln\left[\frac{\tau_{12}}{\tau_a(T)}\right]. \tag{31}$$

Thus, the interlayer resistivity increases logarithmically as the temperature decreases.

We now compare these quantum corrections to the semiclassical conductivity which describes conventional AMRO. The latter is given by[15]

$$\sigma_{\mathrm{conv}}(\mathbf{B}) = \sigma_0\sum_{n=-\infty}^{\infty}\frac{J_n(\gamma\tan\theta)^2}{1+(n\omega_0\tau_{11}\cos\theta)^2}, \tag{32}$$

where $\gamma = ck_F$, $J_n(z)$ is the Bessel function of order n, $\omega_0 = \frac{eB}{m^*}$, and the conductivity at zero field and at $\theta=0$ is

$$\sigma_0 = \frac{2ce^2t_\perp^2m^*\tau_{11}}{\pi\hbar^4}. \tag{33}$$

We can estimate the relative size of the quantum correction to the conventional term as

$$\frac{\sigma_1}{\sigma_0} = \frac{f\left(\frac{e}{\hbar}B_\parallel c\ell\right)}{\pi k_F\ell} \sim \frac{1}{k_F\ell}, \tag{34}$$

for fields such that $eB_\parallel c\ell/\hbar \ll 1$. This indicates that the effects we discuss here are most likely to be seen in "dirty" samples (i.e., short mean-free path) and with a small Fermi surface.

F. Peak in the vicinity of $\theta = \pi/2$

Now, $n_{\max}$ depends on polar angle—as $\theta \to \frac{\pi}{2}$, $B_\perp \to 0$ and hence $n_{\max} \to \infty$. Using the asymptotic expansion of $\psi(x)$ at large x, we obtain (in the limit that $\frac{B_0}{B_a} \sim \frac{\tau_a}{\tau_{11}} \gg 1$)

$$\delta\sigma^C \simeq -\sigma_1\left[\ln\left(\frac{B_0}{B_a}\right) - \frac{B_\perp^2}{24B_a^2}\right]. \tag{35}$$

This correction will have two different dependences on parallel field arising from $f(\frac{e}{\hbar}B_\parallel c\ell)$. At fields much less than $B_p=\hbar/ecl$ it will be independent of parallel field, while for fields larger than B_p it takes the form

$$\delta\sigma^C \simeq -\frac{\sigma_0}{\pi k_F\ell}\frac{B_p}{B_\parallel}\left[\ln\left(\frac{B_0}{B_a}\right) - \frac{B_\perp^2}{24B_a^2}\right]. \tag{36}$$

In the limit that $\theta\to\frac{\pi}{2}$, we can also compare with the limit from $\sigma_{\rm conv}$ which can be obtained by standard saddle-point methods applied to an integral representation of Eq. (32). In the limit that $\gamma\tan\theta\gg 1$,[15]

$$\sigma_{\rm conv} \simeq \sigma_0\frac{B_p}{B_\parallel}\left[1+2\exp\left(-\frac{\pi}{\omega_0\tau_{11}\cos\theta}\right)\sin(2\gamma\tan\theta)\right].$$

If we compare the two contributions in the limit that $\theta\to\frac{\pi}{2}$, for fields larger than B_p, then we find that the size of the quantum correction relative to the semiclassical magnetoconductivity is the same as for the zero-field correction and has the same temperature dependence

$$\frac{\delta\sigma^C}{\sigma_{\rm conv}} \simeq -\frac{1}{\pi k_F\ell}\ln\left[\frac{\tau_{12}}{\tau_a(T)}\right]. \tag{37}$$

In order to compare with experiment, it is useful to separate the conductivity as $\sigma(\mathbf{B})=\sigma_{\rm back}(\mathbf{B})+\Delta\sigma(\mathbf{B})$, where $\sigma_{\rm back}(\mathbf{B})=\sigma_{\rm conv}(\mathbf{B})+\delta\sigma^C(B_\perp=0)$, since it is only the negative magnetoresistance for increasing $B_\perp$ that will be visible. Defining $\rho_{\rm back}=1/\sigma_{\rm back}$, we have

$$\frac{\rho_{zz}}{\rho_{\rm back}} \simeq 1-\frac{\Delta\sigma^C}{\sigma_{\rm back}},$$

which implies a decrease in the resistivity, which grows as $B_\perp$ increases, i.e., as θ deviates from $\frac{\pi}{2}$. In consequence, there will be a peak above the background resistance at $\theta=\frac{\pi}{2}$.

IV. DISCUSSION

The correction to the resistivity at $\theta=\frac{\pi}{2}$, we found in Sec. III, is much smaller in magnitude than the conventional term, but since conventional AMRO are featureless in this region, this quantum contribution can still be visible above the background. The Cooperon should lead to a small peak in the resistivity in the vicinity of $\theta=\frac{\pi}{2}$. The values of θ for which this should be true are those such that both asymptotic formulae hold, i.e., $\cos\theta\ll 1/(ck_F)$ and $B\cos\theta=B_\perp\ll B_a$.

A. Numerical results

We now evaluate the resistivity correction obtained in Sec. III, Eq. (28), for parameters appropriate for α-$(ET)_2KHg(SCN)_4$ (Refs. 1 and 24). Figure 3 shows the calculated temperature dependence and Fig. 4 shows the angular dependence. We calculate the dependence of the interlayer resistivity on temperature, field, and field direction. We choose $k_F=1.4$ nm^{-1}, $\epsilon_F=40$ meV, $\tau_{11}=1$ ps, $\tau_{12}=1.01\tau_{11}$, and $c\simeq 20$ Å. τ_{11} is of the order of the scattering time in the dirty sample considered in Ref. 24, and we choose τ_{12} very close to τ_{11} for our numerics since the visibility of the peak is maximized when $\tau_{11}\sim\tau_{12}$, which implies $\tau_a\sim\tau_\phi$ and grows very large as $T\to 0$. We choose $\tau_a=20$ ps for numerical convenience, which implies $\tau_\phi=25$ ps from Eq. (20). From Eq.

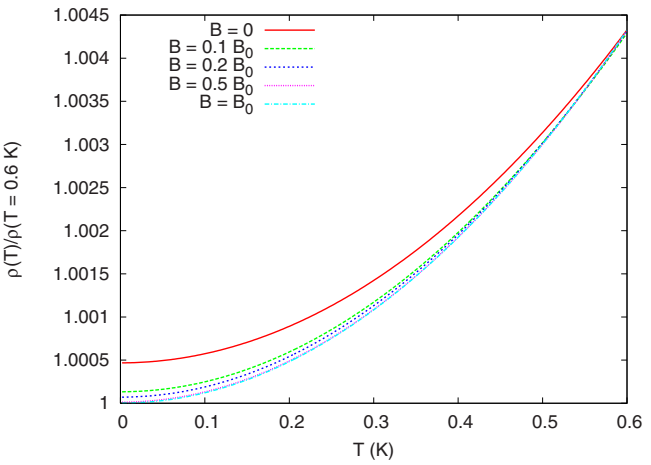

FIG. 3. (Color online) Interlayer resistivity as a function of temperature for several different magnetic fields perpendicular to the layers. In the absence of the field, the resistivity increases logarithmically with temperature due to weak localization effects provided that the inelastic scattering is small enough (in the figure this is masked by the quadratic increase in the resistivity with temperature). As the magnetic field becomes comparable to the field B_0, the feature disappears. The resistivity is normalized to its value at 0.6 K. The parameters used in these plots are $k_F=1.4$ nm^{-1}, $c=2$ nm, $\tau_{11}=1$ ps, $\tau_{12}=1.01\tau_{11}$, $\epsilon_F=40$ meV, and $1/(\tau_\phi(T)/\text{ps})=0.006(T/\text{K})^2$.

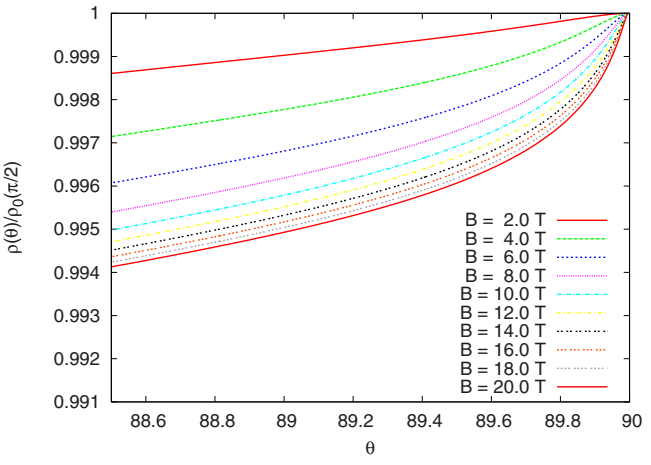

FIG. 4. (Color online) Interlayer resistivity as a function of the angle θ, between the magnetic field and the normal to the layers. The peak at 90 degrees is due to weak localization effects. Note that it is only about 0.5 percent of the total resistivity. The resistivity is normalized to the sum of the semiclassical resistivity and the zero-field quantum correction. As the magnetic field increases from 2 to 20 T, the size of the peak decreases and its width increases. The parameters used in these plots are $k_F=1.4$ nm^{-1}, $c=2$ nm, $\tau_{11}=1$ ps, $\tau_{12}=1.01\tau_{11}$, $\epsilon_F=40$ meV, and $\tau_a=20$ ps.

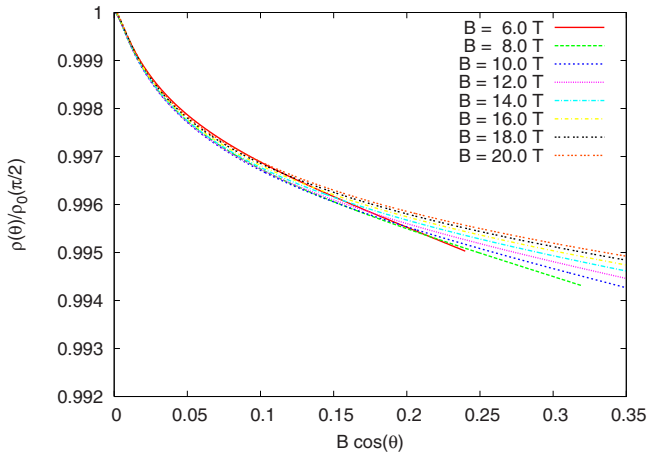

FIG. 5. (Color online) Resistivity data from Fig. 4 plotted as a function of the magnitude of the magnetic field parallel to the layers $B\cos\theta$ for $B > B_p$.

(6) we see that $\tau_\phi \sim 25$ ps at $T \simeq 2.6$ K, so this appears to be a reasonable choice for τ_a. These choices correspond to fields of $B_0 \sim 0.09$ T and $B_a \sim 0.002$ T. The width of the peak is approximately $\Delta\theta = 0.5°$ and the height of the peak is about 0.5% of the background resistance at all fields larger than 2 T.

In Fig. 5 we replot the data from Fig. 4 as a function of $B_\perp = B\cos(\theta)$. It is clear that as B increases, the peak becomes a function of $B_\perp$ only. We determined the width of the peak in two different ways: i) by choosing a fixed value of $\rho(\theta)/\rho(\theta=\frac{\pi}{2})$, and then determining the appropriate $\Delta\theta$ as a function of B, and ii) by subtracting the (nonflat) background and finding the value of $\Delta\theta$ corresponding to the half-maximum of the peak. In case i) $\Delta\theta \sim B^{-1}$ for essentially all values of B, whereas for case ii) $\Delta\theta \sim B^{-1/2}$ for $B \gtrsim B_p \sim 4$ T.

The results in Figs. 5 and 6 are qualitatively in accord with recent experiments on the resistivity in β''-(BEDT-TTF)$_4$[$H_3OCr(C_2O_4)_3$]CH_2Cl_2, in which a peak

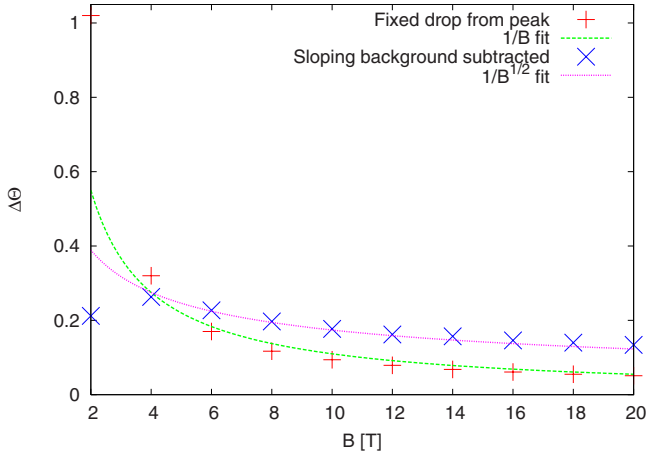

FIG. 6. (Color online) Width of the peak in the resistivity about $\theta = 90°$ as a function of field for the data in Fig. 4. The width is determined either by a fixed drop in the resistance or by subtracting the background. Fits to both procedures are shown, both of which work well for $B > B_p \sim 4$ T.

that depends only on $B\cos(\theta)$ for small θ and a peak width $\Delta\theta \sim 1/B$ were observed.[26] Additionally, features in unpublished data[40] on α-[$(ET)_{1-x}(BETS)_x$]$_2$KHg$(SCN)_4$ with $x \simeq 0.03$ appear to be consistent with the picture presented here.

B. Implications for experiment

Inelastic scattering plays an important role in determining when a resistivity peak will be observed. A reasonable temperature dependence of the inelastic-scattering rate implies that at high temperatures, the inelastic-scattering time is much less than the elastic-scattering time $\tau_\phi \ll \tau_{11}$. At a temperature where the two become comparable, one might expect to see the first hints of a resistance peak which narrows and grows with decreasing temperature until the peak width and height saturate. We expect that there will be a saturation when $1/\tau_a$ reaches its low-temperature limit $\sim[\frac{1}{\tau_{11}} - \frac{1}{\tau_{12}}]$ which is generally nonzero. The visibility of the peak is largest when $\tau_a \gg \tau_{11}$, which will be true when τ_{12} is very close in magnitude to τ_{11}.

In concert with the magnetic-field-dependent signatures discussed above, the temperature and magnetic-field dependence of such a peak in the resistivity should allow it to be distinguished from coherence peaks, whose width and height should have much weaker dependence on temperature and magnetic field.[15] As a consequence, these localization peaks also offer an opportunity to determine the inelastic-scattering rate, independent of regular AMRO which allow a determination of the elastic-scattering rate, and quantum oscillations which allow a determination of the total scattering rate through the Dingle temperature.

Some questions that we have not addressed here but provide interesting avenues for further exploration are with regards to the effects of anisotropy and the coherence of interlayer transport. Our calculation was for an isotropic Fermi surface with isotropic elastic scattering—in general one can expect Fermi-surface properties to vary on different parts of the Fermi surface, which would likely imply that the nature of the peak for parallel fields will also depend on the orientation of the magnetic field within the plane. This might allow the possibility of investigating the inelastic scattering on different parts of the Fermi surface. Second, our derivation assumed weakly incoherent interlayer transport. However, it appears likely to us that similar results should also hold for coherent interlayer transport, and so the presence or absence of this weak localization peak is not necessarily evidence for or against coherent interlayer transport. The visibility of the peak will be stronger in samples with relatively smaller values of $k_F l$, corresponding to smaller values of τ, but the criterion usually used to argue coherence of interlayer transport is comparing the hopping amplitude, $t_\perp$, with the scattering rate $\frac{\hbar}{\tau}$.

We have discussed here the analog of weak localization in the interlayer resistance of layered metals, assuming simple potential scattering. Other scattering mechanisms, such as magnetic impurity scattering, and spin-orbit scattering, can lead to additional contributions to magnetoresistance, such as weak antilocalization in the case of spin-orbit scattering.[32]

The presence of magnetic ions in many β'' organic salts suggests that these should perhaps be considered as possibilities. Magnetic impurity scattering tends to depress the effects of weak localization, but if there is strong spin-orbit scattering, this may lead to additional effects in the vicinity of $\theta=\frac{\pi}{2}$. We are not aware of experiments that exhibit these features, but hope that our work may stimulate investigations in this direction.

V. CONCLUSIONS

In conclusion, we have calculated the effect of the interlayer Cooperon on AMRO in quasi-two-dimensional layered metals. The interlayer Cooperon can give rise to a peak in the magnetoresistance for fields parallel to the layers that behave similarly to conventional weak localization. The features of the peak depend sensitively on magnetic field and the inelastic-scattering time, which should allow it to be distinguished from coherence peaks seen in very low disorder layered metals. This potentially allows for the extraction of information about inelastic scattering in layered metals, and gives another tool with which to learn about the physics of these systems.

ACKNOWLEDGMENTS

The authors thank A. Coldea, R. Joynt, M. Kartsovnik, T. Kawamoto, T. Osada, B. Powell, and J. Singleton for helpful discussions. We are particularly thankful to A. Coldea and M. Kartsovnik for showing us their experimental data prior to publication. M. Smith provided a critical reading of the manuscript. This work was supported by an Australian Research Council Discovery Project grant (R.H.M.), and by NSERC (M.P.K.).

APPENDIX: CALCULATION OF $F(\mathbf{B}_\parallel)$

To calculate $F(\mathbf{B}_\parallel)$ we need to perform an integral over four in-plane disorder-averaged Green's functions

$$F(\mathbf{B}_\parallel) = \int \frac{d^2\mathbf{k}_1}{(2\pi)^2} G^R(\mathbf{k}_1) G^R(-\mathbf{k}_1) \times G^A\left(\mathbf{k}_1 + \frac{ec}{2\hbar}\mathbf{B}_\parallel\right) G^A\left(-\mathbf{k}_1 + \frac{ec}{2\hbar}\mathbf{B}_\parallel\right)$$
$$= \int \frac{d^2\mathbf{k}_1}{(2\pi)^2} \left(\frac{1}{E-\epsilon_k + i\eta}\right)^2 \frac{1}{E-\epsilon_{k-\beta}-i\eta} \times \frac{1}{E-\epsilon_{k+\beta}-i\eta}, \tag{A1}$$

with $\eta=\hbar/2\tau_{11}$, $\epsilon_k=\frac{\hbar^2k^2}{2m^*}$, and $\epsilon_{k-\beta}=\epsilon_k-\sqrt{\frac{2\epsilon_k}{m^*}}\beta\cos\phi+\frac{\beta^2}{2m^*}$, with $\beta=\frac{1}{2}ecB_\parallel$. Rewriting Eq. (A1) as an integral over energy and performing the energy integral using contour integration, we get

$$F(\mathbf{B}_\parallel) = \frac{m^*}{8\pi\hbar^2\eta^3}\int_0^{2\pi} d\phi \left(1-\frac{\beta^2}{4im^*\eta}\cos(2\phi)\right) \times \frac{1}{\left(1-i\frac{\beta^2}{4\eta m^*}+i\frac{\beta\hbar k}{2\eta m^*}\cos\phi\right)^2} \times \left.\frac{1}{\left(1-i\frac{\beta^2}{4\eta m^*}-i\frac{\beta\hbar k}{2\eta m^*}\cos\phi\right)^2}\right|_{\epsilon_k=E+i\eta}. \tag{A2}$$

The second term in the denominators is much smaller than the third term if $\beta \ll 2\hbar k_F$. This corresponds to $B_\parallel \ll 4\hbar k_F/(ec) \sim O(100\mathrm{T})$, which is always satisfied for physically realistic parameters. We then have

$$\mathrm{Re}[F(\mathbf{B}_\parallel)] = -\frac{m^*}{4\hbar^2\eta^3} f\left(\frac{\beta v_F}{\eta}\right). \tag{A3}$$

where

$$f(x) \equiv \frac{1}{2\pi}\int_0^{2\pi} \frac{d\phi}{\left[1+\left(\frac{x}{2}\right)^2\cos^2\phi\right]^2}. \tag{A4}$$

Evaluating this by contour integration gives Eq. (27).

[1] M. V. Kartsovnik, Chem. Rev. (Washington, D.C.) **104**, 5737 (2004).
[2] L. Balicas, S. Nakatsuji, D. Hall, T. Ohnishi, Z. Fisk, Y. Maeno, and D. J. Singh, Phys. Rev. Lett. **95**, 196407 (2005).
[3] C. Bergemann, A. P. Mackenzie, S. R. Julian, D. Forsythe, and E. Ohmichi, Adv. Phys. **52**, 639 (2003).
[4] T. Osada, H. Nose, and M. Kuraguchi, Physica B (Amsterdam) **294-295**, 402 (2001).
[5] U. Beierlein, C. Schlenker, J. Dumas, and M. Greenblatt, Phys. Rev. B **67**, 235110 (2003).
[6] N. E. Hussey, M. Abdel-Jawad, A. Carrington, A. P. Mackenzie, and L. Balicas, Nature (London) **425**, 814 (2003).
[7] M. Abdel-Jawad, M. P. Kennett, L. Balicas, A. Carrington, A. P. Mackenzie, R. H. McKenzie, and N. E. Hussey, Nat. Phys. **2**, 821 (2006).
[8] M. Abdel-Jawad, L. Balicas, M. P. Kennett, R. H. McKenzie, and N. E. Hussey, Physica B (Amsterdam) **403**, 982 (2008).
[9] J. G. Analytis, M. Abdel-Jawad, L. Balicas, M. M. J. French, and N. E. Hussey, Phys. Rev. B **76**, 104523 (2007).
[10] M. Abdel-Jawad, J. G. Analytis, L. Balicas, A. Carrington, J. P. H. Charmant, M. M. J. French, and N. E. Hussey, Phys. Rev. Lett. **99**, 107002 (2007).
[11] M. P. Kennett and R. H. McKenzie, Phys. Rev. B **76**, 054515 (2007).

[12] M. P. Kennett and R. H. McKenzie, Physica B (Amsterdam) **403**, 1552 (2008).
[13] J. Singleton, P. A. Goddard, A. Ardavan, A. I. Coldea, S. J. Blundell, R. D. McDonald, S. Tozer, and J. A. Schlueter, Phys. Rev. Lett. **99**, 027004 (2007).
[14] A. J. Millis, Nature (London) **417**, 599 (2002); T. Valla, P. D. Johnson, Z. Yusof, B. Wells, Q. Li, S. M. Loureiro, R. J. Cava, M. Mikami, Y. Mori, M. Yoshimura, and T. Sasaki, *ibid.* **417**, 627 (2002).
[15] R. H. McKenzie and P. Moses, Phys. Rev. Lett. **81**, 4492 (1998); P. Moses and R. H. McKenzie, Phys. Rev. B **60**, 7998 (1999).
[16] R. N. Bhatt, P. Wölfle, and T. V. Ramakrishnan, Phys. Rev. B **32**, 569 (1985).
[17] N. Dupuis and G. Montambaux, Phys. Rev. Lett. **68**, 357 (1992).
[18] C. Mauz, A. Rosch, and P. Wölfle, Phys. Rev. B **56**, 10953 (1997).
[19] Y. H. Yang, Y. G. Wang, and M. Liu, Phys. Rev. B **64**, 233313 (2001).
[20] G. Bergmann, Phys. Rev. B **39**, 11280 (1989).
[21] W. Szott, C. Jedrzejek, and W. P. Kirk, Phys. Rev. B **45**, 3565 (1992).
[22] O. E. Raichev and P. Vasilopoulos, J. Phys.: Condens. Matter **12**, 589 (2000).
[23] J. Singleton, P. A. Goddard, A. Ardavan, N. Harrison, S. J. Blundell, J. A. Schlueter, and A. M. Kini, Phys. Rev. Lett. **88**, 037001 (2002).
[24] M. V. Kartsovnik, D. Andres, S. V. Simonov, W. Biberacher, I. Sheikin, N. D. Kushch, and H. Müller, Phys. Rev. Lett. **96**, 166601 (2006).
[25] A. I. Coldea, A. F. Bangura, J. Singleton, A. Ardavan, A. Akutsu-Sato, H. Akutsu, S. S. Turner, and P. Day, Phys. Rev. B **69**, 085112 (2004).
[26] A. I. Coldea, P. Goddard, J. Singleton, R. McDonald, A. Akutsu-Sato, H. Akutsu, L. Martin, P. Day, and J. A. Schlueter, Poster and Proceedings, ISCOM 2007 (unpublished).
[27] K. Kechedzhi, V. I. Fal'ko, E. McCann, and B. L. Altshuler, Phys. Rev. Lett. **98**, 176806 (2007).
[28] R. V. Gorbachev, F. V. Tikhonenko, A. S. Mayorov, D. W. Horsell, and A. K. Savchenko, Phys. Rev. Lett. **98**, 176805 (2007).
[29] N. S. Averkiev, L. E. Golub, S. A. Tarasenko, and M. Willander, Phys. Rev. B **64**, 045405 (2001).
[30] J. Rammer, *Quantum Transport Theory* (Perseus, Reading, MA, 1998).
[31] S. Datta, *Electronic Transport in Mesoscopic Physics* (Cambridge University Press, Cambridge, 1995).
[32] S. Hikami, A. I. Larkin, and Y. Nagaoka, Prog. Theor. Phys. **63**, 707 (1980).
[33] B. L. Altshuler, D. Khmel'nitzkii, A. I. Larkin, and P. A. Lee, Phys. Rev. B **22**, 5142 (1980).
[34] M. Y. Simmons, A. R. Hamilton, M. Pepper, E. H. Linfield, P. D. Rose, and D. A. Ritchie, Phys. Rev. Lett. **84**, 2489 (2000).
[35] N. Hanasaki, S. Kagoshima, T. Hasegawa, T. Osada, and N. Miura, Phys. Rev. B **57**, 1336 (1998).
[36] As an aside, we note that another interesting feature of the AMRO in these materials is that they are inverted with respect to the expectation for isotropic interlayer hopping. Such a situation can occur when the interlayer hopping $t_\perp(\phi)$ varies significantly around the Fermi surface in the appropriate way (Ref. 37). It is interesting to note that the planes of ET molecules in adjacent layers are twisted with respect to each other by 62 degrees (Ref. 25), which may be responsible for such an intralayer variation of the interlayer hopping integral.
[37] R. Yagi and Y. Iye, Solid State Commun. **89**, 275 (1994).
[38] T. G. Prokhorova, S. S. Khasanov, L. V. Zorina, L. I. Buravov, V. A. Tkacheva, A. A. Baskakov, R. B. Morgunov, M. Gener, E. Canadell, R. P. Shibaeva, and E. B. Yagubskii, Adv. Funct. Mater. **13**, 403 (2003).
[39] M. A. Tanatar, S. Kagoshima, T. Ishiguro, H. Ito, V. S. Yefanov, V. A. Bondarenko, N. D. Kushch, and E. B. Yagubskii, Phys. Rev. B **62**, 15561 (2000).
[40] M. Kartsovnik (private communication).
[41] B. J. Powell and R. H. McKenzie, J. Phys.: Condens. Matter **18**, R827 (2006).
[42] K. Enomoto, S. Uji, T. Yamaguchi, T. Terashima, T. Konoike, M. Nishimura, T. Enoki, M. Suzuki, and I. S. Suzuki, Phys. Rev. B **73**, 045115 (2006).
[43] M. F. Smith (unpublished).
[44] I. S. Gradshteyn and I. M. Ryzhik, in *Table of Integrals, Series and Products*, 5th ed., edited by A. Jeffrey (Academic, London, 1994).